Available online at www.sciencedirect.com

ScienceDirect

International Journal of Refractory Metals & Hard Materials 26 (2008) 164–172

International Journal of REFRACTORY METALS & HARD MATERIALS

www.elsevier.com/locate/IJRMHM

Wear mechanisms of PVD ZrN coated tools in machining

Deng Jianxin *, Liu Jianhua, Zhao Jinlong, Song Wenlong

Department of Mechanical Engineering, Shandong University, Jinan 250061, Shandong Province, PR China

Received 20 April 2007; accepted 17 May 2007

Abstract

Medium-frequency magnetron sputtered PVD ZrN coatings (ZrN, ZrN/Zr) were deposited on YT15 (WC + 15%TiC + 6%Co) cemented carbide. Microstructural and fundamental properties of these ZrN coatings were examined. Dry machining tests on hardened steel were carried out with these coated tools. The wear surface features were examined by scanning electron microscopy. Results showed that deposition of the PVD ZrN coatings onto the YT15 cemented carbide causes great increase in surface hardness. The ZC-1 coated tool (ZrN/YT15 without interlayer) has the highest surface hardness; while the ZC-2 (ZrN/Zr/YT15 with a Zr interlayer) shows the highest adhesion load for the coatings to the substrate. The ZrN coated tools exhibit improved rake and flank wear resistance to that of the YT15 tool. The coated tools with a Zr interlayer (ZC-2) have higher wear resistance over the one without Zr interlayer (ZC-1). The rake wear of the ZrN coated tools at low cutting speed was mainly abrasive wear; while the mechanism responsible for the rake wear at high cutting speed was determined to be adhesion. Extensive abrasive wear accompanied by small adhesive wear were found to be the predominant flank wear mechanisms for the ZrN coated tools.

Keywords: Coated tools; ZrN; Cutting tools; Wear mechanisms

1. Introduction

Surface coating is an effective method to improve the durability of the materials used in the aggressive environments. By selecting proper coating methods and coating materials, we may prolong the service life of the substrate material and increase the commercial value of the products. New coating deposition techniques developed over the last two decades offer a wide variety of possibilities to tailor surfaces with many different materials and structures. In particular, chemical vapour deposition (CVD) and physical vapour deposition (PVD) techniques have made it possible to deposit thin coatings a few micrometer thick in a temperature range from high temperatures down to room temperature. Ceramic hard coatings are of interest in a number of technological fields due to their physical, chemical and mechanical properties. Coating materials such as TiN, TiC, Al_2O_3 and more recently diamond, diamond-like carbon (DLC) and MoS_2 and their combinations as multilayers have been used with great success [1–4]. Especially, hard nitride coatings are extensively used in many types of cutting operations, where they enhance tool life, improve surface finish and increase productivity [5,6].

The first generation PVD coated tools featured TiN as the hard coating and were applied in interrupted cutting such as milling of steels. The superior performance of PVD TiN coated tools prompted their use in other machining applications, such as turning, as well as in industries as a wear-resistant or protective layer on the dies [7–9]. The continued success of PVD coated tools led to the commercial development of second and third generation PVD coatings (TiCN and TiAlN) which offer even higher machining productivity [10–12].

Recently, zirconium nitride (ZrN) films have attracted increasing interests for various applications, such as diffusion barrier, cryogenic thermometers, decorative coating, hard coatings, because of their high mechanical properties,

* Corresponding author.
E-mail address: jxdeng@sdu.edu.cn (J. Deng).

0263-4368/$ - see front matter © 2007 Elsevier Ltd. All rights reserved.
doi:10.1016/j.ijrmhm.2007.05.009

better corrosion and wear resistance, and exhibiting warmer golden color than the corresponding properties of TiN films [13–18]. ZrN-coated tools have shown significant performance advantages over TiN coated tools during drilling tests [19].

In the present study, medium-frequency magnetron sputtered PVD ZrN coatings were deposited on YT15 (WC + 15%TiC + 6%Co) cemented carbide inserts. Microstructural and fundamental properties of the ZrN coatings were examined. Dry machining tests on hardened steel were carried out with these coated tools. The wear surface features of were examined by scanning electron microscopy, and the wear mechanisms were investigated.

2. Experimental procedures

2.1. Preparation of PVD ZrN coated tools

The substrate material employed for this study was YT15 (WC + 15 wt.% TiC + 6 wt.% Co) cemented carbide. Test pieces of $3 \times 4 \times 36$ (mm) were prepared from the YT15 cemented carbide by cutting and grinding using a diamond wheel and were offered for measurement of flexural strength, Vickers hardness and fracture toughness. Three point bending mode was used to measure the flexural strength over a 30 mm span at a crosshead speed of 0.5 mm/min. Fracture toughness measurement was performed using indentation method in a hardness tester (ZWICK3212) using the formula proposed by Cook and Lawn [20]. On the same apparatus the Vickers hardness was measured on polished surface with a load of 98 N. Data for hardness, flexural strength, and fracture toughness of the YT15 cemented carbide were gathered on five specimens and are listed in Table 1.

The geometry of the substrate to be coated was of ISO SNMG 150412 style inserts of the YT15 cemented carbide. Before deposition the specimens were mirror-polished (1 μm diamonds) and ultrasonically cleaned in acetone and alcohol progressively, each for 5 min, and dried for approximately 20 min in a pre-vacuum dryer. A medium-frequency magnetron sputtering process was employed to deposit the PVD ZrN coatings. The specimens were deposited at 250 °C. A negative bias of −250 V was applied to the substrate during deposition. Ar and N_2 flow were independently controlled using a mass-flow controller. The total gas pressure was kept at 0.5 Pa. The durations for ZrN depositing were 60 min. All the PVD coating conditions are listed in Table 2. The ZrN coating without interlayer is named ZC-1; the ZrN coating with a Zr interlayer is named ZC-2.

Adhesion evaluation of the coatings was made using the scratch test on the MFT-3000 device, by moving the diamond penetrator along the examined specimen's surface with the gradually increasing load. The tests were made with the following parameters: radius of Rockwell diamond stylus 200 μm, load range 0–100 N, load increase rate 100 N/min, penetrator's travel speed 10 mm/min.

The hardness tests of coatings were made on the MH-6 hardness tester. Measurements were made at 0.2 N loads, eliminating influence of the substrate on the measurement results. The film thickness was measured by a surface profilometer. In addition, to verify the obtained results, measurements of the coatings were made also on the cross-sectional view with scanning electron microscope.

2.2. Cutting tests

Cutting tests were carried out on a CA6140 lathe. The cutting tools used were ZrN coated tools (ZC-1 and ZC-2) and uncoated YT15 tools having the following geometry: rake angle $\gamma_o = 5°$, clearance angle $\alpha_o = 5°$, inclination angle $\lambda_s = 5°$, side cutting edge angle $K_r = 75°$. Fig. 1 shows the photos of the ZC-1 and ZC-2 coated tools. For the purpose of comparison, TiN coated tools produced by the authors were also used and the properties of these tools were listed in Table 3 [21].

The workpiece material used was 45# hardened steel (carbon steel, Chinese standard GB699-88) with a hardness of HRC 38-45 in the form of round bar. Its main composition is C 0.42–0.5%, Si 0.17–0.37%, Mn 0.5–0.8%, Ni $\leqslant$ 0.25%, Cr $\leqslant$ 0.25%, Cu $\leqslant$ 0.25%, P $\leqslant$ 0.035%, S $\leqslant$ 0.035%. No cutting fluid was used in the machining processes. All tests were carried out with the following

Table 1
Properties of the YT15 cemented carbide

Composition (wt.%)	Density (g/cm^3)	Hardness (GPa)	Flexural strength (MPa)	Fracture toughness (MPa $m^{1/2}$)	Thermal conductivity (W/(m K))	Thermal expansion Coefficient (10^{-6}/K)
WC + 15% TiC + 6% Co	11.5	15.5	1130.0	12.0	33.47	6.51

Table 2
The PVD coating conditions

Coating temperature (°C)	Total gas pressure (Pa)	N_2 pressure (Pa)	Bias voltage (V)	Cathode current (A)	Coating time (min)	Source to substrate distance (mm)	Power (KW)
250	0.5	0.09	−250	90	60	120	2.5

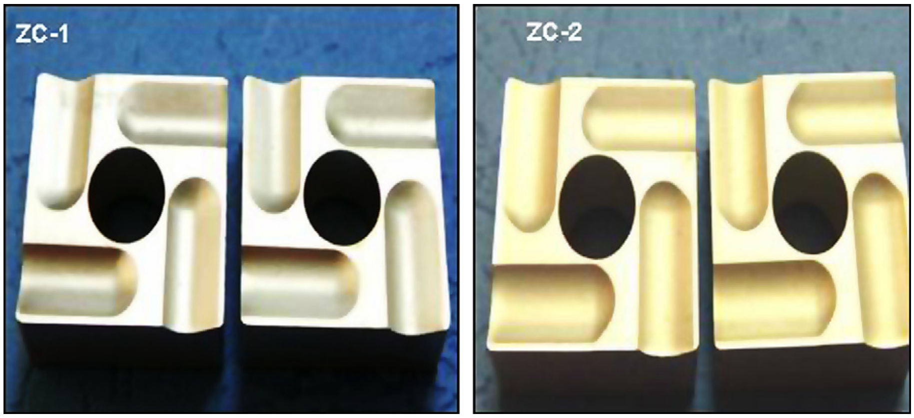

Fig. 1. Photos of the ZC-1 and ZC-2 ZrN coated tools.

Table 3
Properties of the TiN coatings

Substrate	Coating	Hardness (GPa)	Critical load (N)	Coating thickness (μm)
YT15 cemented carbide	TiN	25.5	64.0	4.2

parameters: depth of cut $a_p = 0.2$ mm, feed rate $f = 0.1$ mm/r, cutting speed $v = 60–360$ m/min.

Tool flank wear was measured using a ×20 optional microscope system linked via transducers to a digital read out. The worn rake and flank regions on the tools were examined using scanning electron microscopy.

3. Results and discussion

3.1. ZrN coating microstructures and adhesion evaluation

Hardness, critical load, and coating thickness of the investigated ZrN coatings are presented in Table 4. It was revealed that the uncoated YT15 cemented carbide has a hardness of 15.5 GPa (see Table 1). Deposition of the PVD coatings onto the specimens causes the surface layer hardness increase. The hardness of ZC-1 (without interlayer) reaches 28.0 GPa, that is up to 80.0% more compared to that of YT15 substrate; while the hardness of ZC-2 (with a Zr interlayer) shows a little decrease (26.8 GPa) compared with that one without interlayer.

The critical load characterizing the adherence of the coating to the substrate was determined as the one corresponding to the acoustic emission (AE) increase signalling beginning of spalling of the coating in scratch test (Fig. 2).

Table 4
Properties of the ZrN coatings

Code name	Substrate	Coating	Hardness (GPa)	Critical load (N)	Coating thickness (μm)
ZC-1	YT15	ZrN	28.0	65.0	4.0
ZC-2	YT15	ZrN + Zr	26.8	72.5	5.4

It was found that the critical load of ZC-2 is about 72.5 N; while the critical load of ZC-1 shows a little decrease (65.0 N) compared with that of ZC-2 (see Table 4), which reveals that Zr interlayer between ZrN and YT15 substrate can improve interface adhesion. The effect of Ti interlayer on the residual stress inside ZrN coated tools was analyzed [21]. It is indicated that the Ti interlayer can decrease the residual stress at interface of the coated tools. Therefore, the improvement of interface adhesion of ZC-2 with a Zr interlayer may be attributed to the decrease of residual stress.

Fig. 3 shows the SEM micrograph of the cross-sectional image of the ZrN coating (ZC-1). It shows a dense and fine grained coating structure, the coating thickness is about 4.0 μm. Fig. 4 illustrates the X-ray diffraction analysis of the ZrN coating. It is noted that ZrN existed in the coated surface.

3.2. Cutting performance of the ZrN coated tools

Fig. 5 shows the flank wear of ZC-1 and ZC-2 ZrN coated tools, TiN coated tool, and YT15 uncoated tool

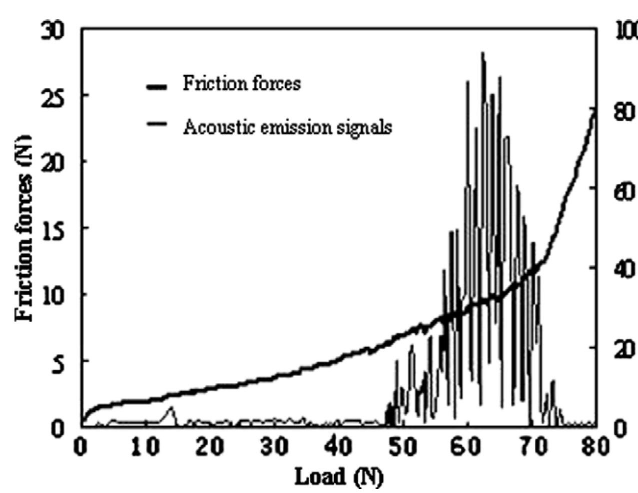

Fig. 2. The friction forces and acoustic emission signals of ZC-2 sample in scratch test.

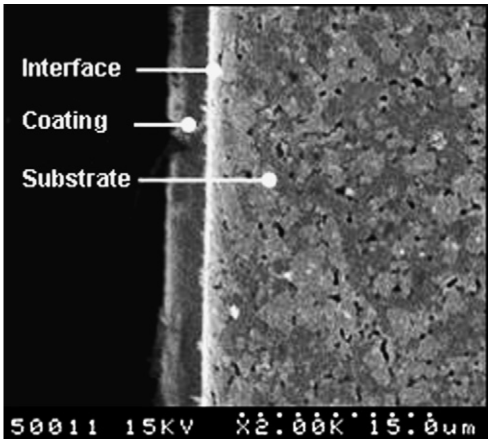

Fig. 3. SEM micrograph of the cross-sectional image of ZrN coating (ZC-1).

in dry machining of 45# hardened steel at conditions of $v = 150$ m/min, $a_p = 0.2$ mm, $f = 0.1$ mm/r. It is indicated that the ZrN coated tools showed more flank wear resistance compared with that of TiN coated tool and YT15 tool under the same test conditions. The ZrN coated tool with a Zr interlayer (ZC-2) exhibited the lowest flank wear; while the uncoated YT15 tool showed the highest flank wear.

Fig. 6 illustrates the resultant force F_z, radial thrust force F_y, and axial thrust force F_x as a function of cutting speeds in dry cutting of 45# hardened steel. From this figure, it was found that the F_z, F_y, and F_x of ZrN coated tools are smaller than that of the YT15 tool under the same cutting conditions.

As can be seen from Tables 1, 3, and 4, the ZrN coated tools have high hardness than that of the uncoated YT15 and TiN coated tool. In addition, the ZC-2 (with a Ti interlayer) shows improved interface adhesion and great coating thickness compared with that of ZC-1 and TiN coated tool. Therefore, the higher flank wear resistance of the ZC-2 coated tool may correspond to its higher hardness, improved interface adhesion and great film thickness.

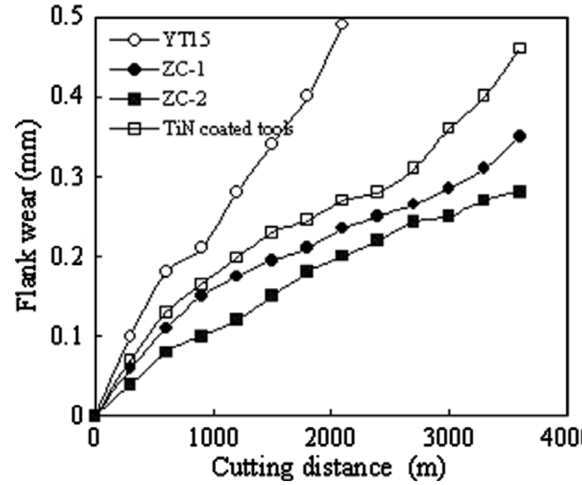

Fig. 5. Flank wear of ZrN coated tools, TiN coated tools, and YT15 uncoated tool in dry machining of 45# hardened steel ($v = 150$ m/min, $a_p = 0.2$ mm, $f = 0.1$ mm/r).

3.3. Rake wear of the ZrN coated tools

Fig. 7a and b shows the SEM micrographs of the worn rake surface of YT15 tool in machining of 45# hardened steel at cutting speed of 100 m/min and 200 m/min respectively. It reveals quite a number of cracks on the worn rake face when at cutting speed of 100 m/min (Fig. 7a). When

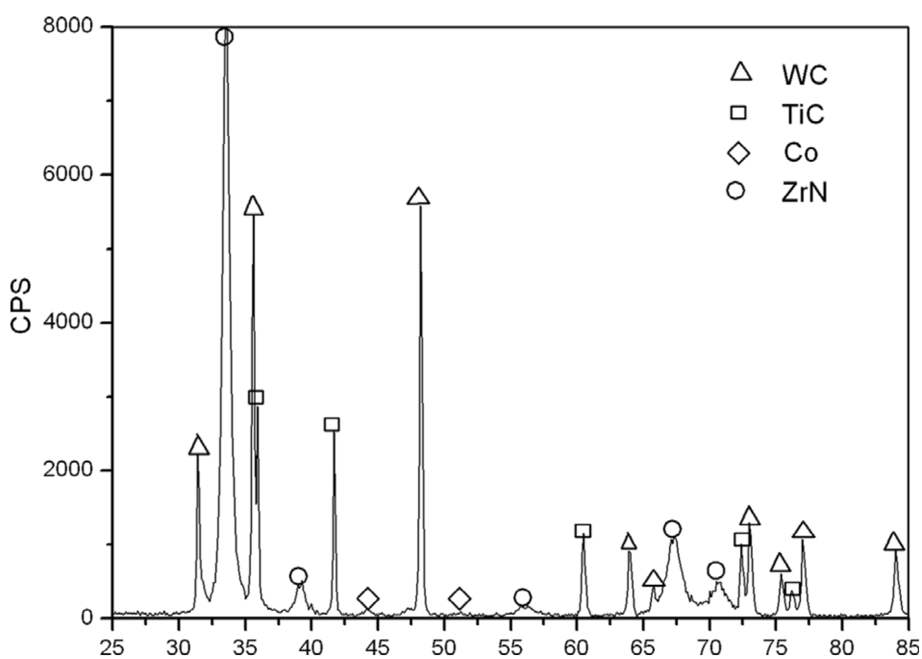

Fig. 4. X-ray diffraction analysis of the ZrN coating.

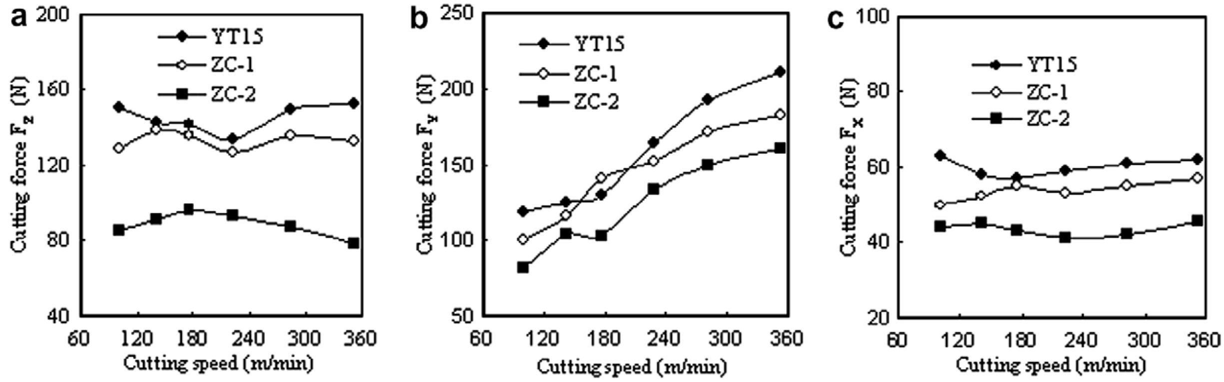

Fig. 6. Effect of cutting speed on the cutting forces for ZrN coated tools and YT15 tool in dry cutting of 45# hardened steel, (a) resultant force F_z, (b) radial thrust force F_y, and (c) axial thrust force F_x.

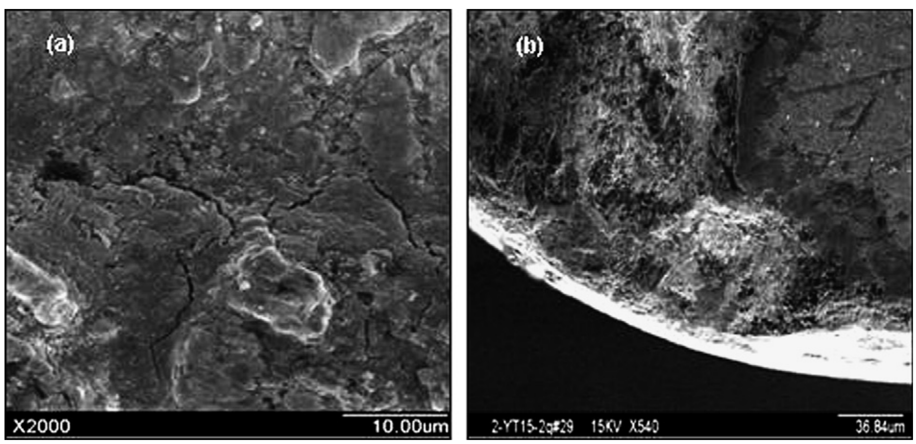

Fig. 7. SEM micrographs of the worn rake surface of YT15 tool in machining of 45# hardened steel at cutting speed of (a) 100 m/min and (b) 200 m/min after 8 min operation.

these cracks spread, chipping of a large area on the tool rake face may be occurred. At high cutting speed (200 m/min), the whole tool tip was broken down completely (Fig. 7b).

Fig. 8a illustrates the SEM micrograph of the worn rake face of ZC-1 coated tool in machining of 45# hardened steel at a cutting speed of 100 m/min. The coating near the cutting edge at the tool rake face is severely worn. The SEM micrograph of the rake wear track at higher magnification is illustrated in Fig. 8b. From this figure, groove and ridge marks are clearly evident on the worn rake face for ZC-1 coated tools.

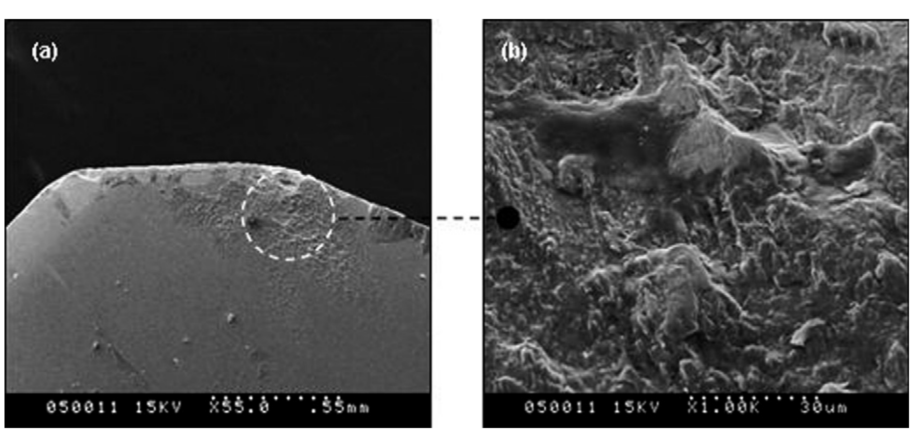

Fig. 8. SEM micrographs of the worn rake surface of ZC-1 coated tool in machining of 45# hardened steel at cutting speed of 100 m/min after 8 min operation.

Typical tool wear on the rake face of ZC-2 coated tool in machining of 45# hardened steel at a cutting speed of 100 m/min is shown in Fig. 9, which reveals small chipping at the cutting edges. Compared with YT15 and ZC-1 (see Figs. 7 and 8), the ZC-2 coated tools exhibited relatively small wear on the rake face.

Typical tool wear on the rake face of ZC-1 coated tool at high cutting speed (200 m/min) is shown in Fig. 10. The wear track near the cutting edge shows clearly of adhering materials smeared on the rake face (Fig. 10b and c). These adhered materials were identified by EDX analysis, and the results are shown in Fig. 10d. It is indicated that the adhered materials contain mainly Fe elements.

Fig. 11a illustrates the SEM micrograph of the worn rake surface of ZC-2 coated tool at high cutting speed (200 m/min). The SEM micrograph of the rake wear track at higher magnification is shown in Fig. 11b, which reveals the existence of a thin film on the worn rake face, and this

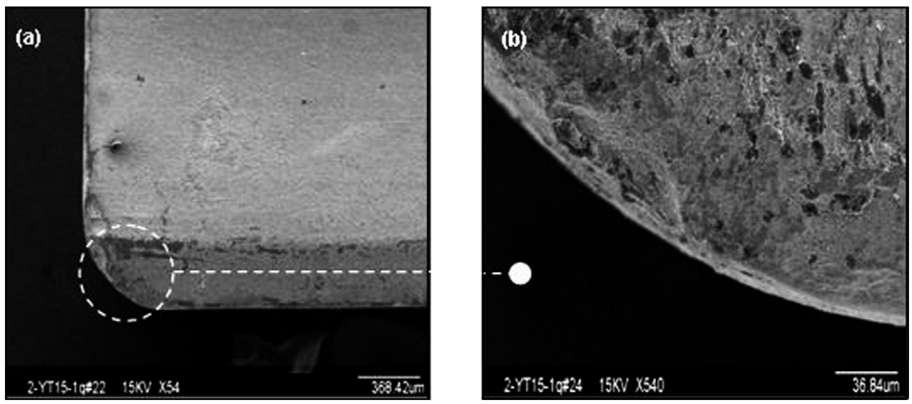

Fig. 9. SEM micrographs of the worn rake surface of ZC-2 coated tool in machining of 45# hardened steel at cutting speed of 100 m/min after 8 min operation.

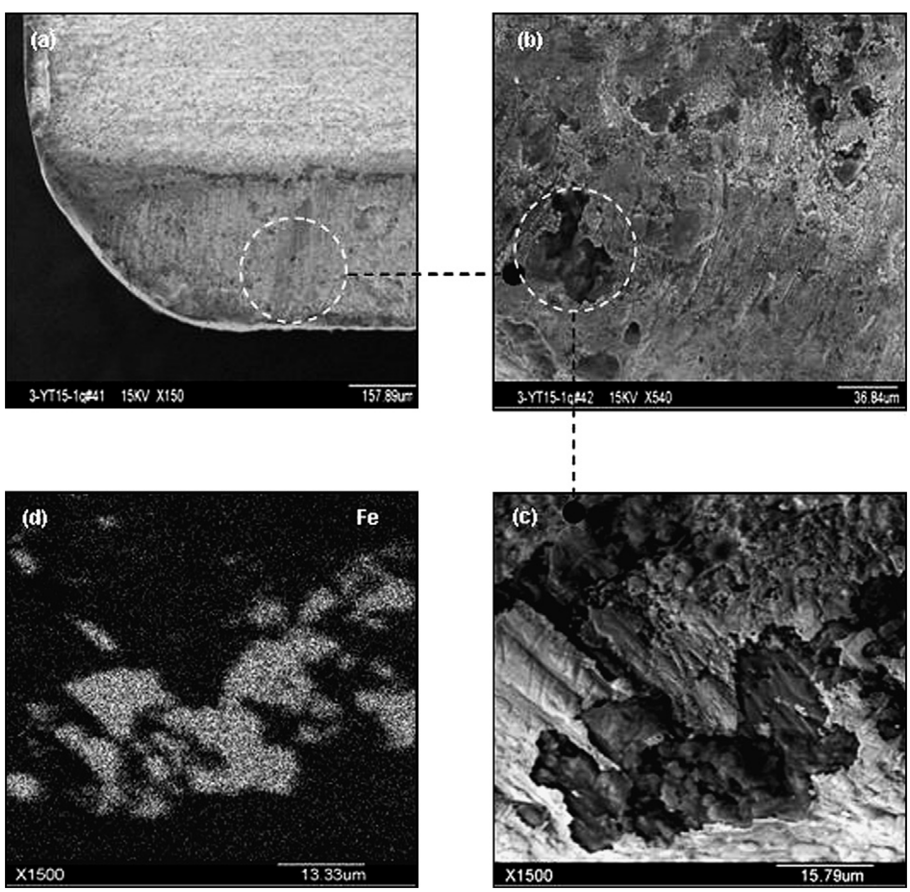

Fig. 10. SEM micrographs of the worn rake surface of ZC-1 coated tool at cutting speed of 200 m/min after 8 min operation.

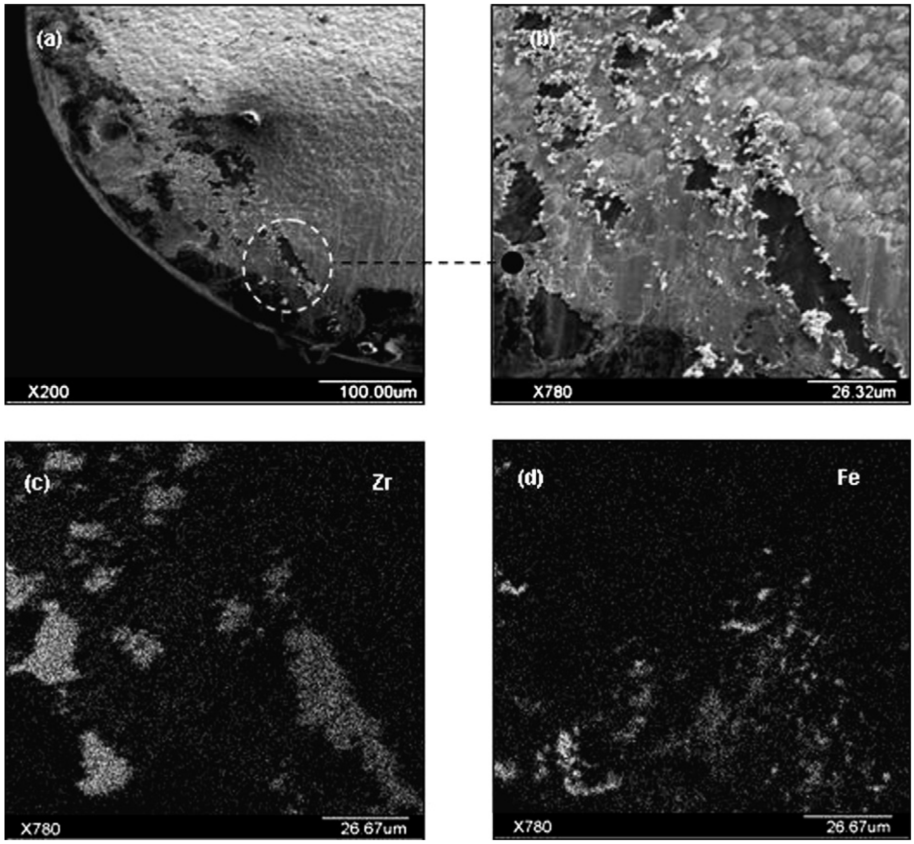

Fig. 11. SEM micrographs of the worn rake surface of ZC-2 coated tool at cutting speed of 200 m/min after 8 min operation.

film was broken in some areas. EDX map of the distribution of Zr and Fe elements on the wear track is shown in Fig. 11c and d, respectively. The results indicated that the thin film contains mainly Fe elements; while Zr elements of the ZC-2 coatings were identified in the broken areas. Thus, the workpiece materials have been smeared on the rake face under high speed cutting conditions.

3.4. Flank wear of the ZrN coated tools

Fig. 12a shows the typical flank wear track of the YT15 tool in machining of 45# hardened steel at a cutting speed of 200 m/min. It is noted that the tool tip and the cutting edge were fractured. Closer examination at higher magnification of the flank wear of YT15 tool is shown in Fig. 12b. Cracks are clearly evident on the flank wear surfaces. The probability of finding such features on the flank wear surface is significantly greater.

Typical flank wear track of ZC-1 tool in machining of 45# hardened steel at a cutting speed of 200 m/min is shown in Fig. 13. It is noted that the wear land is not of uniform width, ridges and mechanical plowing grooves are clearly evident on the flank wear surfaces, and it is indicative of typical abrasive wear. It is also revealed

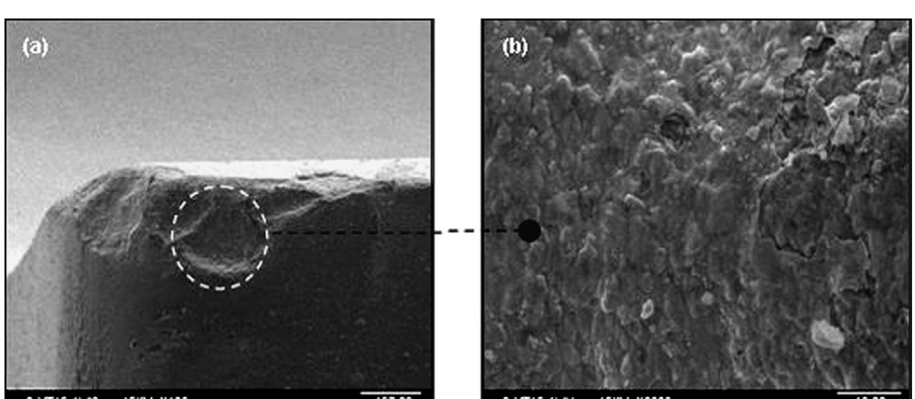

Fig. 12. SEM micrographs of the flank wear surface of YT15 tool in machining 45# hardened steel at cutting speed of 200 m/min after 8 min operation.

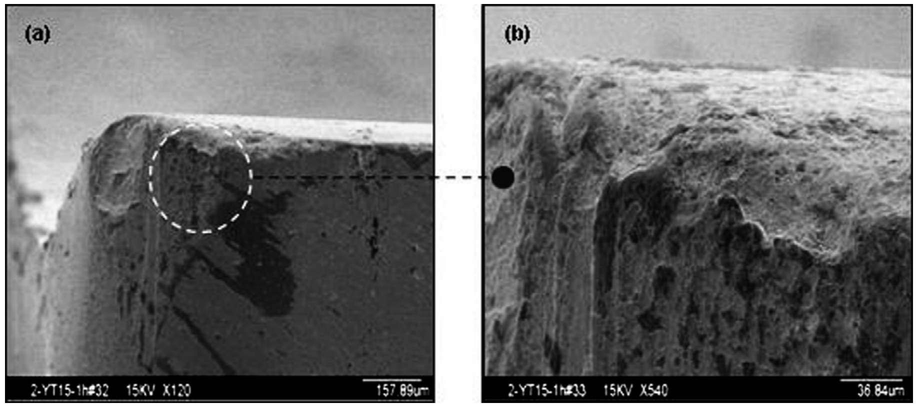

Fig. 13. SEM micrographs of the flank wear surface of ZC-1 coated tool in machining 45# hardened steel at cutting speed of 200 m/min after 8 min operation.

that some adhering materials were smeared on the flank face. EDX identification shows that these adhered materials contain mainly Fe elements. Similar features were also found for ZC-2 tool. Compared with YT15 tool, the ZrN coated tool exhibited small flank wear under the same test conditions. Therefore, extensive abrasive wear accompanied by small adhesive wear were found to be the predominant flank wear mechanisms for the ZrN coated tools.

3.5. Discussion

Different modes of tool failure including abrasive wear, adhesive wear, and coating breakage were observed when machining of hardened steel with ZrN coated tools. Among these tool wear patterns, abrasive wear was found to be the main mode of flank wear, while adhesive wear were the main rake face wear types. It is common that several tool wear patterns may appear simultaneously at the same time and have an effect on each other.

The uncoated YT15 tools exhibit less rake wear resistance to that of the ZrN coated tools in machining of hardened steel, and the rake face of the uncoated YT15 tools was cracked or fractured both at low and high cutting speed (see Fig. 7). As can be seen from Tables 1 and 4, the uncoated YT15 tools have lower hardness than that of the ZrN coated tools. Also the cutting forces of the YT15 tools are higher than that of the ZrN coated tools under the same cutting conditions (see Fig. 6). At high cutting speed conditions, there is high cutting temperature at the vicinity of the tool tip. The hardness of the YT15 tool materials may decrease at high cutting temperatures, which aggravates the abrasive wear on tool rake face. High cutting temperature also resulted in diffusion, adhesion, plastic deformation, etc. The tool–chip contact length is shorter in high cutting speed than at conventional cutting speed, which causes the cutting force to be concentrated adjacent to the tool tip. Therefore, the less rake wear resistance of uncoated YT15 tools may correspond to its low hardness and great cutting forces.

Abrasive wear is usually a dominant wear mechanism on the flank face, it is also observed on the rake face of ZrN coated tools (see Fig. 8). Abrasion is characterized by development of grooves and ridges in the direction of tool sliding against a newly machined surface of the work piece or chip sliding against the rake face. In many cases, the abrasive action may also be attributed to special features of the flowing chip, which is characterized by a serrated profile along its edges. This type of serrated chips abrades the tool rake face and creates scars in the rake wear surface. High stresses generated at the tool–chip interface during machining may also cause plastically deformed grooves and ridges on rake faces.

The rake wear of the ZrN coated tool is different from crater wear in conventional cutting. In the conventional cutting, the tool wear on the rake face occurred in the form of a crater, which was formed at some distance from the cutting edge, while the rake wear of the ZrN coated tool on rake face was adjacent to the cutting edge. Actually, the maximum wear on the rake face occurred on the main cutting edge (see Figs. 8–11). As ZrN has high hardness, good chemical inertness, and better corrosion. The ZrN coatings at the tool rake face acted as wear resistance layer, and resulted in a decrease in crater wear.

The rake wear of the ZrN coated tools at low cutting speed was mainly abrasive wear; while at high speed cutting conditions, the workpiece materials have been smeared on the rake face of ZrN coated tools (see Figs. 10 and 11). The repeated adhering of the workpiece material to the tool and breaking away from the tool after adhesion, initiate the loss of the coating from the rake face. Adhesive wear of the ZrN coated tool also involves the mechanism in which coatings or their small aggregates are pulled out of the tool surface and are carried away at the underside of the chip or torn away by the adherent work piece.

4. Conclusions

Medium-frequency magnetron sputtered PVD ZrN coatings were deposited on YT15 cemented carbide. Dry machining tests on hardened steel were carried out with these coated tools. The main conclusions obtained can be summarised as follows:

1. Deposition of the PVD ZrN coatings onto the YT15 cemented carbide causes great increase in surface hardness. The ZC-1 coated tool (ZrN/YT15 without interlayer) has the highest surface hardness; while the ZC-2 (ZrN/Zr/YT15 with a Zr interlayer) shows the highest adhesion load for the coatings to the substrate.
2. The ZrN coated tools exhibit improved rake and flank wear resistance to that of the YT15 tool. The coated tools with a Zr interlayer (ZC-2) have higher wear resistance over the one without Zr interlayer (ZC-1).
3. The rake wear of the ZrN coated tools at low cutting speed was mainly abrasive wear; while the mechanism responsible for the rake wear at high cutting speed was determined to be adhesion.
4. Extensive abrasive wear accompanied by small adhesive wear were found to be the predominant flank wear mechanisms for the ZrN coated tools.

Acknowledgements

This work was supported by "the National Natural Science Foundation of China (50475133, 50675120)", and "the Program for New Century Excellent Talents in University (NCET-04-0622)".

References

[1] Klocke F, Krieg T. Coated too1s for metal cutting features and applications. Ann CIRP 1999;48(2):515–25.
[2] Prengel HG, Pfouts WR, Santhanam AT. State of the art in hard coatings for carbide cutting tools. Surf Coat Technol 1998;102:183–90.
[3] Uhlmann E, Lachmund U, Brücher M. Wear behavior of HFCVD-diamond coated carbide and ceramic tools. Surf Coat Technol 2000;131:395–9.
[4] Renevier NM, Lobiondo N, Fox VC, Teer DG, Hampshire J. Performance of MoS_2/metal composite coatings used for dry machining and other industrial applications. Surf Coat Technol 2000;123:84–91.
[5] Ducros C, Benevent V, Sanchette F. Deposition, characterization and machining performance of multilayer PVD coatings on cemented carbide cutting tools. Surf Coat Technol 2003;163–164:681–8.
[6] Kalss W, Reiter A, Derflinger V, Gey C, Endrino JL. Modern coatings in high performance cutting applications. Int J Refract Met Hard Mater 2006;24(5):399–404.
[7] Ezugwu EO, Okeke CI. Tool life and wear mechanisms of TiN coated tools in an intermittent cutting operation. J Mater Process Technol 2001;116(1):10–5.
[8] Soković M, Bahor M. On the inter-relationships of some machinability parameters in finish machining with cermet TiN (PVD) coated tools. J Mater Process Technol 1998;78(1–3):163–70.
[9] Fenske GR. Nitride and carbide coatings for high speed steel cutting tools. Tribol Trans 1989;32:339–45.
[10] Sahin Y, Sur G. The effect of Al_2O_3, TiN and Ti(C,N) based CVD coatings on tool wear in machining metal matrix composites. Surf Coat Technol 2004;179:349–55.
[11] Jindal PC, Santhanam AT, Schleinkofer U, Shuster AF. Performance of PVD TiN, TiCN, and TiAlN coated cemented carbide tools in turning. Int J Refract Met Hard Mater 1999;17(1–3):163–70.
[12] Harris SG, Doyle ED, Vlasveld AC. Influence of chromium content on the dry machining performance of cathodic arc evaporated TiAlN coatings. Wear 2003;254(1–2):185–94.
[13] Pilloud D, Dehlinger AS, Pierson JF, Roman A, Pichon L. Reactively sputtered zirconium nitride coatings: structural, mechanical, optical and electrical characteristics. Surf Coat Technol 2003;174–175:338–44.
[14] Atar Erdem, Sabri Kayali E, Cimenoglu Huseyin. Sliding wear behaviour of ZrN and (Zr, 12 wt% Hf)N coatings. Tribol Int 2006;39:297–302.
[15] Budke E, Krempel-Hesse J, Maidhof H, Schussler H. Decorative hard coatings with improved corrosion resistance. Surf Coat Technol 1999;112:108–13.
[16] Ramos Henry J, Valmoria Nicomedes B. Thin-film deposition of ZrN using a plasma sputter-type negative ion source. Vacuum 2004;73:549–54.
[17] López G, Staia MH. High-temperature tribological characterization of zirconium nitride coatings. Surf Coat Technol 2005;200(7):2092–9.
[18] Brugnoni C, Lanza F, Macchi G, Müller R, Parnisari E, Stroosnijder MF. Evaluation of the wear resistance of ZrN coatings using thin layer activation. Surf Coat Technol 1998;100–101:23–6.
[19] Gariboldi E. Drilling a magnesium alloy using PVD coated twist drills. J Mater Process Technol 2003;134(3):287–95.
[20] Cook RF, Lawn BR. A modified indentation toughness technique. J Am Ceram Soc 1983;66(11):200–1.
[21] Liu Jianhua, Development of ZrN coated tools and study on their friction and wear behaviours. PhD dissertation, Shandong University, 2007.